

STRUCTURE AND PROPERTIES OF AlMgSi ALLOYS AFTER ECAP AND POST-ECAP AGEING

STRUKTURA IN LASTNOSTI ZLITIN AlMgSi, STARANIH PRED ECAP IN PO NJEM

Martin Fujda¹, Miloš Matvija¹, Tibor Kvačkaj², Ondrej Milkovič¹, Pavol Zubko¹,
Katarína Nagyová¹

¹Department of Materials Science, Faculty of Metallurgy, Technical University of Košice, Slovakia

²Department of Metals Forming, Faculty of Metallurgy, Technical University of Košice, Slovakia
martin.fujda@tuke.sk

Prejem rokopisa – received: 2012-02-10; sprejem za objavo – accepted for publication: 2012-03-22

The mechanical properties and the microstructures of the EN AW 6082 and EN AW 6063 aluminium alloys subjected to pre-ECAP solutionizing heat treatment, equal channel angular pressing (ECAP), and post-ECAP artificial ageing are compared. The quenched alloy states were severely deformed at room temperature by the ECAP technique following route B_C. Repetitive ECAP caused formation of the ultra-fine subgrain microstructure with a high dislocation density and high strain hardening of the alloys, thus exhibiting an improvement in strength, but also a degradation of the analysed alloys' ductility. The application of the optimal artificial-ageing regimes after a severe plastic deformation improved only the tensile ductility of the alloys, while their strength was slightly decreased because the softening effect caused by the solid-solution recovery and the relaxation of the internal stress dominated over the hardening effect caused by the expected metastable β'' - and β' -Mg₂Si phase precipitation during the artificial ageing treatment.

Keywords: aluminium alloys, ECAP, ageing, microstructure, mechanical properties

Primerjali smo lastnosti EN AW 6082 in EN AW 6063 aluminijevih zlitin, raztopno žarjenih pred stiskanjem skozi pravokotni kanal (ECAP), po stiskanju ECAP in umetno staranih po ECAP-postopku. Zlitine v gašenem stanju so bile močno deformirane pri sobni temperaturi s tehniko ECAP po poti B_C. Ponovljena ECAP je povzročila nastanek ultra drobnoprzate podmikrostrukture z veliko gostoto dislokacij, velikim utrjevanjem zlitin in s tem povečanje trdnosti ter poslabšanje duktilnosti preiskovanih zlitin. Optimalni režim umetnega staranja po veliki plastični deformaciji je povzročil samo izboljšanje natezne duktilnosti materiala, njihova trdnost pa je bila zmanjšana zaradi učinka mehčanja pri popravi trdne raztopine in sproščanju notranjih napetosti, ki prevladujejo nad učinkom utrjevanja z izločanjem izločkov metastabilne β'' - in β' -Mg₂Si faze med postopkom umetnega staranja.

Ključne besede: aluminijeve zlitine, ECAP, staranje, mikrostruktura, mehanske lastnosti

1 INTRODUCTION

At present, the equal-channel angular pressing (ECAP) technique is a very effective method of severe plastic deformation, and has been widely used for producing ultra-fine grain microstructures of Al-based alloys with significantly improved mechanical properties, including enhanced superplasticity, high strength, etc.¹⁻¹⁰ The severe plastic deformation (SPD) made by the ECAP process also markedly increases the density of lattice defects in the solid solution, and can thus accelerate the precipitation process of the strengthening particles during the post-ECAP ageing treatment applied to the age-hardenable aluminium alloys.¹¹⁻¹³ However, the ultra-fine-grained age-hardenable alloys often exhibit low tensile ductility at room temperature. Therefore, it is important to obtain ductility comparable to that of the conventional coarse-grained age-hardenable Al-based alloys.

EN AW 6063 and 6082 are the most used AlMgSi alloys that are suitable for different miscellaneous structural applications in the building, automotive and aircraft industries due to their strength-modification

options, low density, good corrosion properties, and good weldability.^{14,15} The optimal combination of heat treatment and the SPD by repetitive ECAP led to a significantly increased strength and a relatively good ductility of these alloys caused by the ultra-fine grained structure formation and the strengthening precipitation of the β' -Mg₂Si phase particles during the post-ECAP ageing treatment.^{4,16-21}

The aim of the present work is to investigate the effect of the SPD by repetitive ECAP and the subsequent artificial ageing on the microstructure and the mechanical properties of the EN AW 6082 and EN AW 6063 aluminium alloys.

2 EXPERIMENTAL WORK

The experiments were carried out on the EN AW 6082 and EN AW 6063 aluminium alloys, the chemical composition of which is presented in **Table 1**. The analyzed alloys in the form of extruded rods, subjected to artificial ageing (T5 temper), were used as the initial states. Prior to the deformation in an ECAP die, the specimens of the initial states were solution annealed for

1.5 h at 550 °C (6082 alloy) or at 510 °C (6063 alloy) and subsequently cooled to room temperature by water quenching. The purpose of these heat-treatment regimes was to obtain a supersaturated solid solution.

Table 1: Chemical composition of the EN AW 6082 and EN AW 6063 aluminium alloys (w/%)

Tabela 1: Kemijska sestava aluminijevih zlitin EN AW 6082 in EN AW 6063 v masnih deležih (w/%)

| alloy | Mg | Si | Mn | Fe | Zn | Cu | Al |
|------------|------|------|------|------|------|------|------|
| EN AW 6082 | 0.60 | 1.0 | 0.49 | 0.21 | 0.02 | 0.06 | bal. |
| EN AW 6063 | 0.44 | 0.52 | 0.03 | 0.21 | 0.02 | 0.03 | bal. |

The quenched specimens were subjected to a deformation in an ECAP die with a channel intersection angle $\Phi = 90^\circ$, and an arc of curvature $\Psi = 37^\circ$ up to 4 (6082 alloy) or 6 passes (6063 alloy), respectively. The repetitive ECAP of the specimens of size $\phi = 10 \text{ mm} \times 100 \text{ mm}$ was realized at room temperature following route B_C (the sample was rotated in the same sense by 90°). After ECAP, the specimens were subjected to artificial ageing in the temperature range of 60–180 °C as a function of time to determine the post-ECAP artificial-ageing condition for the highest peak hardness.

The microstructures of the investigated alloys obtained after quenching, deformation in the ECAP die, and after the post-ECAP peak-ageing treatment were analyzed in the central zones of the specimens' cross-sections using a transmission electron microscopy (TEM). The samples for TEM were prepared from the 1-mm-thick slices that were ground and polished to a thickness of about 0.15 mm. These slices were finally electrolytically thinned in a solution of 25 % HNO₃ and 75 % CH₃OH at a temperature of -30°C . The average grain size of the solid solution for all the analysed alloy states was determined according to ASTM E112.

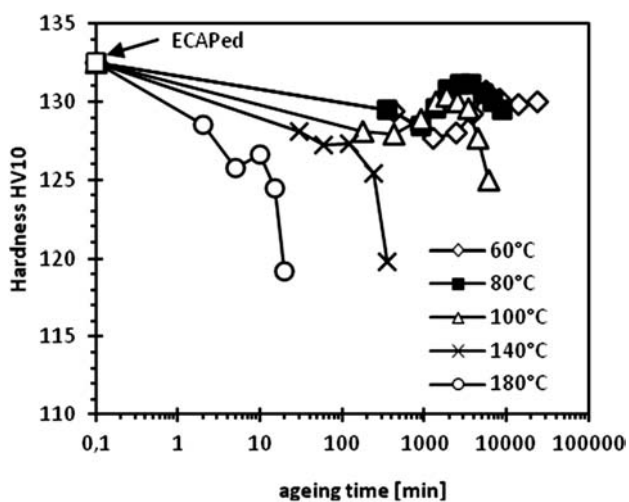


Figure 1: Vickers hardness of the ECAPed EN AW 6082 alloy state as a function of artificial ageing time at various ageing temperatures

Slika 1: Vickersova trdota zlitine EN AW 6082 po ECAP kot funkcija časa umetnega staranja pri različnih temperaturah staranja

The influence of the severe plastic deformation by the ECAP process and post-ECAP artificial ageing on the mechanical properties of the analyzed alloys was evaluated with the Vickers hardness measurement (HV 10) and a tensile test. The tensile test (the initial strain rate of $2.5 \times 10^{-4} \text{ s}^{-1}$) was carried out on short specimens ($d_0 = 5 \text{ mm}$, $l_0 = 10 \text{ mm}$) made from quenched, ECAP-processed and post-ECAP peak-aged alloy billets. Subsequently, the characteristics of the strength ($R_{p0.2}$ – yield strength and R_m – tensile strength), the uniform tensile elongation (A_g), the tensile elongation (A), and the reduction in the area (Z) were determined.

3 RESULTS AND DISCUSSION

3.1 Hardness

The Vickers hardness of the analyzed alloy states is summarized in **Table 2**. **Figures 1 and 2** show the variation of the Vickers hardness of the ECAPed analyzed alloys as a function of artificial ageing time at a temperature range of 60–180 °C. A significant increase in the alloys' hardness value (by about 120 % for the 6082 alloy and about 202 % for the 6063 alloy) was achieved by the ECAP processing of the quenched alloy states. A post-ECAP artificial-ageing treatment was applied to increase the hardness of the ECAPed alloys. The ECAPed alloy state reached peak hardness after about 60 h of the artificial ageing at 80 °C, but the

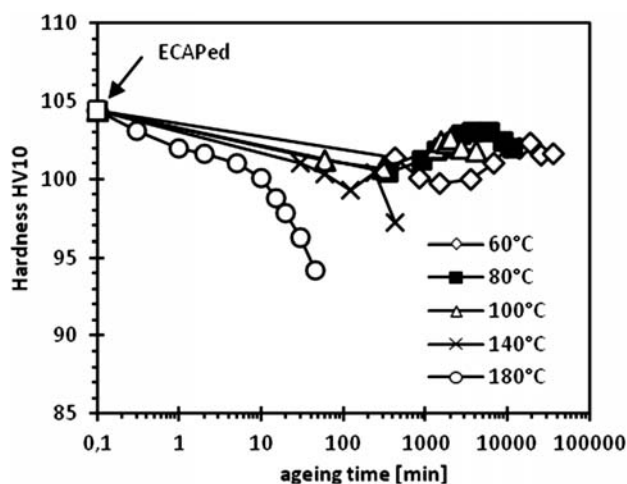


Figure 2: Vickers hardness of the ECAPed EN AW 6063 alloy state as a function of artificial ageing time at various ageing temperatures

Slika 2: Vickersova trdota zlitine EN AW 6063 po ECAP kot funkcija časa umetnega staranja pri različnih temperaturah staranja

Table 2: Vickers hardness of the analyzed alloy states

Tabela 2: Vickersova trdota analiziranih stanj zlitin

| alloy/state | Q | E | post-ECAP peak-aged | | | | |
|-------------|------|-------|---------------------|-------|--------|--------|--------|
| | | | 60 °C | 80 °C | 100 °C | 140 °C | 180 °C |
| EN AW 6082 | 60.2 | 132.5 | 130.7 | 131.1 | 130.5 | 127.3 | 126.6 |
| EN AW 6063 | 34.6 | 104.4 | 102.3 | 103.0 | 102.6 | 100.4 | – |

Q-quenched, E-ECAPed

maximum values were only slightly lower (by about 1.4 HV) than those of the ECAPed alloy states. The increase of the ageing temperature from 60 °C to 100 °C resulted in the peak-ageing-time shortening. However, the maximum alloys' hardness was the highest after being aged at 80 °C. During the post-ECAP ageing at higher temperatures (140 °C and 180 °C), the hardness of the ECAPed alloy states was decreased in a very short time.

3.2 Microstructure

Figure 3 shows the recrystallized microstructure of the 6082-alloy quenched state that consists of fine solid-solution grains (average size: 14.6 μm). However, very coarse grains (average size: 115.6 μm) of the recrystallized solid solution were observed after the quenching of the 6063 alloy (**Figure 4**).

In the case of the 6082 alloy (containing the mass fraction 0.49 % of Mn), no considerable solid-solution

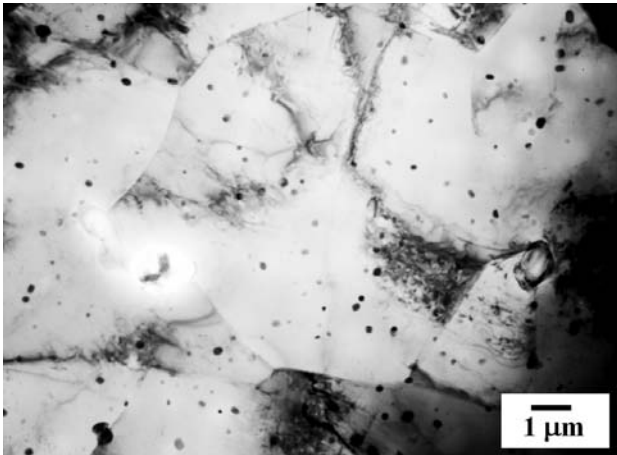


Figure 3: Microstructure of the quenched EN AW 6082 alloy state (550 °C + water quenching), TEM

Slika 3: Mikrostruktura gašene zlitine EN AW 6082 (550 °C + gašenje v vodi), TEM

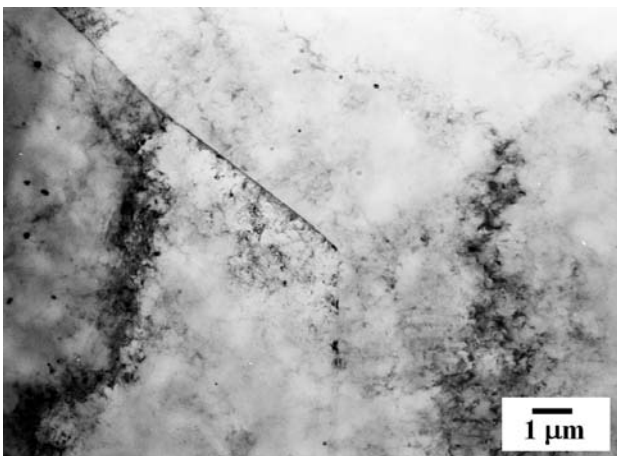


Figure 4: Microstructure of the quenched EN AW 6063 alloy state (510 °C + water quenching), TEM

Slika 4: Mikrostruktura gašene zlitine EN AW 6063 (510 °C + gašenje v vodi), TEM

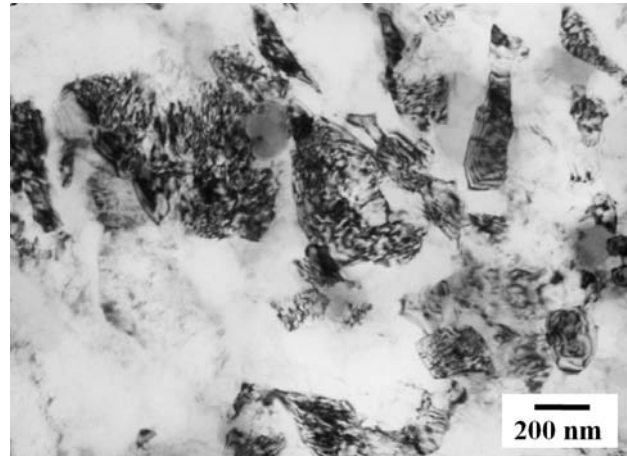


Figure 5: Microstructure of the ECAPed EN AW 6082 alloy state, TEM

Slika 5: Mikrostruktura zlitine EN AW 6082 po ECAP, TEM

grain growth during the applied solution annealing at 550 °C was prevented by the grain-boundary pinning effect of the fine, dispersive, Mn-rich phase particles (**Figure 3**; particle size: 30–300 nm). The role of these dispersive particles is to inhibit the recrystallization process and the matrix grain growth.^{22–25} Comparing **Figures 3** and **4**, it is obvious that the volume fraction of the fine dispersive particles in the coarse-grained matrix of the 6063 alloy (Fe-rich phase particles with the average size of 150 nm) was lower than in the 6082-alloy matrix. Both types of dispersive particles were mostly distributed homogeneously throughout the equiaxed solid-solution grains, which exhibited a relatively low dislocation density in both quenched alloy states.

During the repetitive ECAP applied to the quenched alloy state, the solid-solution grains were heterogeneously refined. A cell-dislocation substructure, equiaxed ultra-fine subgrains, and high dislocation

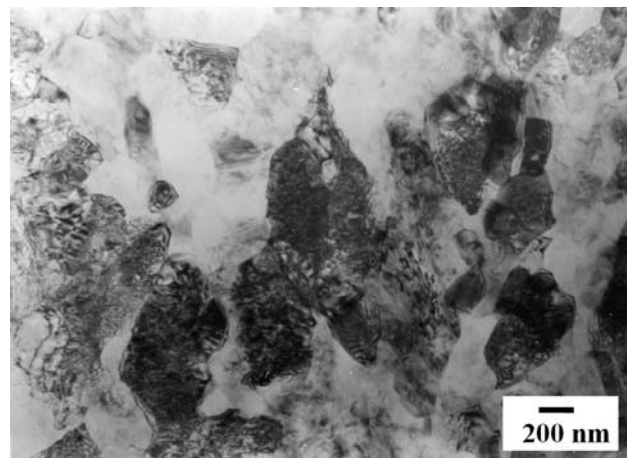


Figure 6: Microstructure of the post-ECAP aged EN AW 6063 alloy treated for 60 h at 80 °C, TEM

Slika 6: Mikrostruktura zlitine EN AW 6063 po ECAP, starane 60 h pri 80 °C, TEM

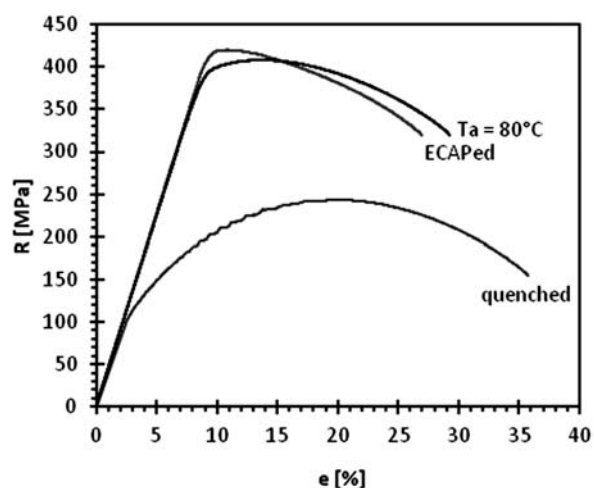


Figure 7: Stress-strain curves of the EN AW 6082 alloy states
Slika 7: Krivulja napetost – raztezek za različna stanja zlitine EN AW 6082

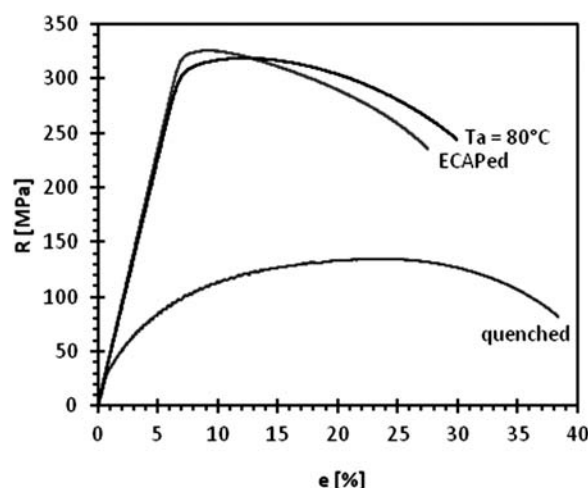


Figure 8: Stress-strain curves of the EN AW 6063 alloy states
Slika 8: Krivulja napetost – raztezek za različna stanja zlitine EN AW 6063

density within the subgrains were observed in the microstructure of the ECAPed alloys (**Figure 5**). The average subgrain size (180 nm) measured for the ECAPed 6082 alloy was a little bit smaller than the size of the subgrains (220 nm) of the quenched 6063-alloy state formed during ECAP. This was a result of the supersaturation of the severely deformed solid solution, obtained for the quenched 6082 alloy prior to the use of repetitive ECAP that was higher than that obtained for the 6063 alloy with lower Mg and Si contents. With an increase in the content of the alloying elements in the solid solution of the Al-based alloys, the microstructure formed after ECAP becomes finer and the dislocation density inside the ultrafine grains is higher.²⁶ After the peak ageing of the ECAPed alloy states (**Figure 6**), a slight dislocation recovery was observed in the subgrains, still having a very high dislocation density, and in the dislocation cells. In addition, the ultra-fine subgrains grew to a size of about 250 nm and 280 nm during the peak ageing of the 6082 and 6063 alloys, respectively.

3.3 Tensile test

The values of the tensile strength (R_m), the yield strength ($R_{p0.2}$) and the tensile ductility (A_g , A , Z), which are presented in **Table 3**, and the stress-strain curves shown in **Figures 7** and **8**, provide a comparison of the mechanical properties determined for the quenched, ECAPed and post-ECAP peak-aged (for 60 h at 80 °C) states of the analyzed alloys. An elimination of the strengthening effect of the nanoparticles of the β'' - and β' -Mg₂Si phases through their dissolution into the solid solution of the quenched alloy states is indicated by their low yield strength, ultimate tensile strength and high ductility. The ultimate tensile strength and, especially, the yield stress of the quenched alloy states increased significantly ($R_{p0.2}$ by about 293MPa and 283 MPa for the 6082 and 6063 alloys, respectively) due to the

repetitive ECAP, while the tensile ductility (A , Z) deteriorated. The tensile-deformation behaviour of these deformed alloy states (**Figures 7** and **8**) is typical for the severely strain-hardened (ECAPed) AlMgSi alloys^{19,21} for which the low values of the uniform tensile elongation (A_g) and a high $R_{p0.2}/R_m$ ratio have been found.

Despite the fact that the hardness values of the post-ECAP peak-aged alloy states are only a little bit lower than those of the ECAPed ones, the yield strength and the ultimate tensile strength of the ECAPed alloys decreased by about 5.5 % and 2.5 %, respectively, during the applied peak-ageing treatment. It is obvious that the applied ageing of the ECAPed alloys resulted in an improved tensile ductility (mainly the uniform tensile elongation A_g). This softening of the alloys occurred because the softening effect caused by the microstructure low recovery and the relaxation of the internal stresses dominates the hardening effect caused by the expected sequence precipitation of the metastable Mg₂Si-phase (GP-zones, β'' - and β' -phase) particles.^{27,28}

Table 3: Mechanical properties of the analyzed alloy states

Tabela 3: Mehanske lastnosti analiziranih stanj zlitin

| Alloy | State | $R_{p0.2}/$ MPa | $R_m/$ MPa | $A_g/$ % | $A/$ % | $Z/$ % |
|------------|-------|--------------------|---------------|-------------|-----------|-----------|
| EN AW 6082 | Q | 115 | 243 | 14.1 | 31.9 | 72.5 |
| | E | 408 | 420 | 1.6 | 19.8 | 39.8 |
| | pEa | 384 | 408 | 4.7 | 22.1 | 42.7 |
| EN AW 6063 | Q | 34 | 135 | 20.2 | 36.4 | 86.5 |
| | E | 317 | 326 | 2.3 | 22.5 | 43.1 |
| | pEa | 300 | 319 | 5.2 | 24.5 | 42.9 |

Q-quenched, E-ECAPed, pEa-post-ECAP aged

4 CONCLUSIONS

The severe plastic deformation of the quenched EN AW 6082 and EN AW 6063 aluminium alloys realized

with the ECAP process caused a refinement and an intensive strain hardening of the alloy solid solution. The result was the increased hardness and strength of the alloys and, on the other hand, a decrease in the alloys' tensile ductility. The increased supersaturation of the severely deformed solid solution obtained for the quenched 6082 alloy was a reaction to its higher strengthening caused by the ECAP processing and was higher than that obtained for the 6063 alloy with the lower Mg and Si contents. The artificial post-ECAP peak-ageing of the alloys was effective only in slightly improving the tensile ductility of the ECAPed alloys, which was a consequence of the low recovery of the ECAPed alloy and the relaxation of internal stresses.

Acknowledgements

This work was supported by the Scientific Grant Agency of the Slovak Republic within the grant project VEGA No. 1/0866/09.

5 REFERENCES

- ¹ V. M. Segal, V. I. Reznikov, A. E. Drobyshevskiy, V. I. Kopylov, *Russian Metallurgy*, 1 (1981), 99–105
- ² M. Furukawa, Z. Horita, M. Nemoto, T. G. Langdon, *Journal of Materials Science*, 36 (2001), 2835–2843
- ³ J. Bidulská, R. Kočíško, R. Bidulský, M. Actis Grande, T. Donič, M. Martikán, *Acta Metallurgica Slovaca*, 16 (2010), 4–11
- ⁴ Z. Horita, T. Fujinami, M. Nemoto, T. G. Langdon, *Journal of Materials Processing Technology*, 117 (2001), 288–292
- ⁵ R. K. Islamgaliev, N. F. Yunusova, R. Z. Valiev, N. K. Tsenev, V. N. Perevezentsev, T. G. Langdon, *Scripta Materialia*, 49 (2003), 467–472
- ⁶ S. Lee, M. Furukawa, Z. Horita, T. G. Langdon, *Materials Science and Engineering, A* 342 (2003), 294–301
- ⁷ R. Z. Valiev, N. A. Enikeev, T. G. Langdon, *Metallic Materials*, 49 (2011), 1–9
- ⁸ Z. Horita, S. Lee, S. Ota, K. Neishi, T. G. Langdon, *Materials Science Forum*, 357–359 (2001), 471–476
- ⁹ K. Turba, P. Malek, M. Cieslar, *Metallic Materials*, 45 (2007), 165–170
- ¹⁰ M. J. Starink, N. Gao, M. Furukawa, Z. Horita, C. Xu, T. G. Langdon, *Reviews on Advanced Materials Science*, 7 (2004), 1–12
- ¹¹ W. J. Kim, C. S. Chung, D. S. Ma, S. I. Hong, H. K. Kim, *Scripta Materialia*, 49 (2003), 333–338
- ¹² M. Y. Murashkin, M. V. Markushev, Y. V. Ivanisenko, R. Z. Valiev, *Solid State Phenomena*, 114 (2001), 91–96
- ¹³ J. K. Kim, W. J. Kim, *Solid State Phenomena*, 124–126 (2007), 1437–1440
- ¹⁴ T. Kvačkaj, R. Bidulský (Eds.), *Aluminium Alloys, Theory and Applications*, InTech, Rijeka 2011
- ¹⁵ J. R. Davis (Ed.), *Aluminium and Aluminium Alloys*, ASM Specialty Handbook, ASM International, Ohio 1993
- ¹⁶ J. Zrník, Z. Nový, T. Kvačkaj, V. Bernáček, D. Kešner, M. Slámová, *Acta Metallurgica Slovaca*, 10 (2004), 277–284
- ¹⁷ B. Cherukuri, T. S. Nedkova, R. Srinivasan, *Materials Science and Engineering, A* 410–411 (2005), 394–397
- ¹⁸ J. C. Werenskiold, H. J. Roven, *Materials Science and Engineering, A* 410–411 (2005), 174–177
- ¹⁹ H. J. Roven, H. Nesboe, J. C. Werenskiold, T. Seibert, *Materials Science and Engineering, A* 410–411 (2005), 426–429
- ²⁰ P. Leo, E. Cerri, P. P. De Marco, H. J. Roven, *Journal of Materials Processing Technology*, 182 (2007), 207–214
- ²¹ W. J. Kim, J. Y. Wang, *Materials Science and Engineering, A* 464 (2007), 23–27
- ²² N. Parson, J. Hankin, K. Hicklin, C. Jowett, Comparison of the extrusion performance and product characteristics of three structural extrusion alloys: AA6061, AA6082 and AA6005A, In.: *Proceedings of the 7th International Aluminium Extrusion Technology Seminar*, Vol. 1, Aluminium Association, Washington DC, 2000, 1–12
- ²³ G. F. Vander Voort (Ed), *Metallography and Microstructures*, ASM Handbook, Vol. 9, ASM International, Ohio 2004
- ²⁴ A. L. Dons, *Journal of Light Metals*, 1 (2001), 133–149
- ²⁵ L. Lodgaard, N. Ryum, *Materials Science and Engineering, A* 283 (2000), 144–152
- ²⁶ J. May, M. Dinkel, D. Amberger, H. W. Höppel, M. Göken, *Metallurgical and Materials Transactions, A* 38 (2007), 1941–1945
- ²⁷ M. Hockauf, L. W. Meyer, D. Nickel, G. Alisch, T. Lampke, B. Wielage, L. Krüger, *Journal of Materials Science*, 43 (2008), 7409–7417
- ²⁸ K. Hockauf, L. W. Meyer, M. Hockauf, T. Halle, *Journal of Materials Science*, 45 (2010), 4754–4760